PCR-based detection in a micro-fabricated platform†

Shantanu Bhattacharya,‡[a,b] Shuaib Salamat,[a,b] Dallas Morisette,[c] Padmapriya Banada,[d] Demir Akin,[a,e] Yi-Shao Liu,[a,b] Arun K. Bhunia,[d] Michael Ladisch[e] and Rashid Bashir*§[a,b,e]

Received 8th February 2008, Accepted 23rd April 2008
First published as an Advance Article on the web 23rd May 2008
DOI: 10.1039/b802227e

We present a novel, on-chip system for the electrokinetic capture of bacterial cells and their identification using the polymerase chain reaction (PCR). The system comprises a glass–silicon platform with a set of micro-channels, -chambers, and -electrodes. A platinum thin film resistor, placed in the proximity of the chambers, is used for temperature monitoring. The whole chip assembly is mounted on a Printed Circuit Board (PCB) and wire-bonded to it. The PCB has an embedded heater that is utilized for PCR thermal cycle and is controlled by a Lab-View program. Similar to our previous work, one set of electrodes on the chip inside the bigger chamber (0.6 μl volume) is used for diverting bacterial cells from a flowing stream into to a smaller chamber (0.4 nl volume). A second set of interdigitated electrodes (in smaller chamber) is used to actively trap and concentrate the bacterial cells using dielectrophoresis (DEP). In the presence of the DEP force, with the cells still entrapped in the micro-chamber, PCR mix is injected into the chamber. Subsequently, PCR amplification with SYBR Green detection is used for genetic identification of *Listeria monocytogenes* V7 cells. The increase in fluorescence is recorded with a photomultiplier tube module mounted over an epifluorescence microscope. This integrated micro-system is capable of genetic amplification and identification of as few as 60 cells of *L. monocytogenes* V7 in less than 90 min, in 600 nl volume collected from a sample of 10^4 cfu ml^{-1}. Specificity trials using various concentrations of *L. monocytogenes* V7, *Listeria innocua* F4248, and *Escherichia coli* O157:H7 were carried out successfully using two different primer sets specific for a regulatory gene of *L. monocytogenes*, *prfA* and 16S rRNA primer specific for the *Listeria* spp., and no cross-reactivity was observed.

Introduction

Microbial pathogens pose a serious threat to humans, and their rapid and accurate detection is very important for food safety and medical diagnostics. Although several conventional methods for detection of pathogenic microorganisms and their toxins exist and are currently being applied, nevertheless, utilization of chip-based techniques has obvious advantages in terms of enhanced speed of detection, automation, and point-of-care use.[1–6] Detection of bacterial pathogens is critical to a wide range of applications in food safety, industrial microbiology, homeland security, public health, and clinical diagnostics. Detection assays must be sensitive and specific, and capable of detecting low concentrations of target species without the interference with background materials. Although many chemical detectors can detect chemical agents at levels that pose a risk to human health, biological detectors can only rarely detect microorganisms directly from samples at or below human risk levels.[7] For example, as few as 50–80 cells of *Escherichia coli* O157:H7 are sufficient to cause an infection and probably much lower numbers can trigger an inflammatory response.[8] A related challenge is the fact that the target microorganisms, at times, are present in very low concentrations and either the target has to be amplified by culture methods, or else enough of a sample volume has to be flowed through the device so as to concentrate the microorganisms and bring their number up to a detection threshold. Active concentration methods such as centrifugation, mechanical filtration,[9] immunomagnetic separations,[10] or dielectrophoresis (DEP)[11,12] have been reported. Cabrera and Yeager have presented a microfluidic flow cell for bacterial concentration utilizing electrokinetic effects.[13] Hu *et al.*[14] have demonstrated cell sorting by modulating the dielectrophoretic amplitude response with particles differing in their polarization. Grodinzki *et al.*[15] have presented a micro-fabricated system for cell concentration and genetic sample

[a]*Birck Nanotechnology Center, Purdue University, West Lafayette, IN, USA*
[b]*School of Electrical and Computer Engineering, Purdue University, West Lafayette, IN, USA*
[c]*BioVitesse Inc., West Lafayette, IN, USA*
[d]*Molecular Food Microbiology Laboratory, Purdue University, West Lafayette, IN, USA*
[e]*Weldon School of Biomedical Engineering, Purdue University, West Lafayette, IN, USA*

† Electronic supplementary information (ESI) available: Description of the control apparatus and the optical detection setup, supplementary figures and fluorescence data. See DOI: 10.1039/b802227e

‡ Present address: Department of Mechanical Engineering, IIT Kanpur, India.

§ Present address: Micro and Nanotechnology Laboratory, Department of Electrical and Computer Engineering & Bioengineering, University of Illinois at Urbana-Champaign, Urbana, IL, USA. E-mail: rbashir@uiuc.edu

preparation from complex sample backgrounds. Genetic analysis on a microfuidic chip by integrating DNA amplification and capillary electrophoresis, in purified DNA samples, has been demonstrated by Mastrangelo and co-workers[16] and Mathies et al.[17] Real-time PCR on purified *stx1* (150 bp) of *E. coli* samples has been performed on-chip using TaqMan PCR.[18] Although other isothermal DNA/RNA amplification techniques, such as *in-situ* amplification,[19] LAMP amplification (loop-mediated amplification), TMA (transcription-mediated amplification),[20] SDA (strand displacement amplification), RCA (rolling circle amplification), NASBA (nucleic acid sequence-based amplification),[21] *etc.*, have been developed, these techniques have not yet been applied to on-chip architecture. PCR and RT-PCR, on the other hand, are still amongst the most popular techniques for nucleic acid amplification due to their simplicity, low assay time, high selectivity and ease of translating onto the chip.[21] On-chip sample concentration using DEP-based capture and off-chip PCR have also been demonstrated. Neilsen *et al.*[22] demonstrated the purification of a baker's yeast sample by removing PCR inhibitors like bovine hemoglobin and heparin. Other RNA detection techniques like hybridization assays using fluorophores have been attempted at the microchip scale.[20] However, the fact that RNA as a molecule is highly unstable,[23] which makes detection protocols extremely difficult. Lagally *et al.*[24] have shown DEP-based cell trapping with hybridization-based RNA detection of 60 *E. coli* MC1061 cells. Aspects of specificity and selectivity of targets were not addressed in their work. Earlier, our group reported the design and development of a biochip with integrated capabilities of DEP-based cell diversion and trapping followed by impedance-based detection of the bacterial growth.[12] In our present work, we build on the previous device platform and demonstrate a DEP-assisted bacterial cell trapping and PCR-based detection with high sensitivity and specificity. Our system is capable of detecting a minimum of 60 cells of *Listeria monocytogenes* V7 in a volume of 600 nl using PCR amplification with SYBR Green detection. Specificity of the assay depended on the selection of target genes; *prfA* (508 bp) and 16S rRNA (400 bp) from *L. monocytogenes* V7 over *L. innocua* F4248 or *E. coli* O157:H7. All the amplification results were further verified using gel electrophoresis.

Dielectrophoresis for cell concentration

The phenomenon of dielectrophoresis is observed when neutral or charged particles (such as bacterial cells with their overall negative charge) are placed in a non-uniform electric field applied to the electrodes. Particles will move towards the electrodes independently of the direction of the applied field. This movement is determined by the dielectric properties (conductivity and permittivity) of the particles and not simply by their charge, as is the case in the more widely known phenomenon of electrophoresis.[25] The time-averaged dielectrophoresis force F for a dielectric sphere immersed in a medium is valid for all particles in the effective moment approximation, and is given by

$$F = 2\pi\varepsilon_0\varepsilon_m r^3 \mathrm{Re}[f_{CM}]\nabla |E_{rms}|^2 \quad (1)$$

where ε_0 is the vacuum dielectric constant, ε_m is the dielectric constant of the media, r is the particle radius, E_{rms} is the root mean square value of the electric field, and $\mathrm{Re}[f_{CM}]$ is the real part of the well-known Claussius–Mossotti factor,[26]

$$f_{CM} = (\varepsilon_p^* - \varepsilon_m^*)/(\varepsilon_p^* + 2\varepsilon_m^*) \quad (2)$$

where ε_p^* and ε_m^* are the relative complex permittivity of the particle and the medium respectively and are each given by $\varepsilon^* = \varepsilon + \sigma/(j\omega)$, where ε is the permittivity, σ is the conductivity of the particle or medium, $j = \sqrt{-1}$, and ω is the angular frequency.

The polarizability of a particle (and therefore the direction and magnitude of the dielectrophoretic force) varies as a function of the magnitude and frequency of the applied electric field.[27] Besides, the polarizability of particles and media also depend on their dielectric constant and conductivity.[28] Therefore, a transition from positive to negative DEP may occur just by changing the frequency of the AC field. The frequency at which this transition occurs, is referred to as the cross-over frequency.[27] In the case of bacterial cells, the cross-over frequency is a strong function of the permittivity of the medium. For media with a conductivity smaller than the cell conductivity (44 mS m^{-1}), f_{CM} is positive for frequencies less than 1 MHz. Therefore using a low conductivity growth medium (low permittivity), the bacterial cells can be trapped over the microelectrodes.[29]

Materials and methods

Bacterial cultures and culture conditions

L. monocytogenes ATCC 23074 transformed with pNF8, a GFP-encoding plasmid was used to demonstrate on-chip DEP capture of cells. The cells were grown in LCGM (Low Conductivity Growth Medium) (BioVitesse Inc., San Jose, CA)[29] containing 10 μg ml^{-1} of erythromycin at 37 °C, for 18–20 h. The final cell numbers were detected by serial dilution and plating on brain heart infusion (BHI) agar. The culture was diluted, plated, and counted using the Gel Doc™ (M/s Biorad) and Image-J software.

Polymerase chain reaction (PCR)

The PCR was carried out on-chip using a qPCR kit with SYBR Green detection (M/s Qiagen Inc.). 50 μl of PCR mix was prepared by mixing 25 μl of qPCR supermix, 16 μl of nuclease-free water, 5 μl of template (intact bacterial cells), and 2 μl of diluted SYBR Green solution (SYBR Green : nuclease-free water = 1 : 1000). 1 μl (0.5 uM) of each primer (forward and reverse) for 508 bp *prfA* amplicon, specific to *L. monocytogenes* V7, was used.[30] The sequences for these primers are 5′-CGGGATAAAACCAAAACAATTT-3′ (forward) and 5′-TGAGCTATGTGCGATGCCACTT-3′ (reverse). The performance regulatory factor A (*prfA*) gene is responsible for regulation of virulence genes in *L. monocytogenes*. The reaction was carried out in a GeneAmp® PCR system 9700 (Applied Biosystems, Foster City, CA). A parallel experiment using similar conditions was also carried out using the purified template DNA in real-time ABI Prism System 7500 (Applied Biosystems, Foster City, CA). The sensitivity of the method was evaluated by using various concentrations of bacteria, ranging from 10^4 to 10^8 cfu ml^{-1}, thus varying the concentration of the initial DNA template. Selectivity tests of the primer sets for *prfA* gene and 16S rRNA were performed for *L. monocytogenes* V7,

L. innocua F4248, and *E. coli* O157:H7, existing as a mono- or mixed-culture to mimic the natural scenario. Amplification was verified off-chip by gel electrophoresis using 1.2% agarose in 1X TAE buffer.

Device design

A silicon-based microfluidic biochip was fabricated for testing the proposed detection scheme. The design and fabrication of the first biochip was described in detail in our earlier work.[12] The overall design concept is based on a large straight channel (main channel) through which the sample can be flowed at the desired rate while the cells contained within it are deviated by dielectrophoretic (DEP) forces into the small chamber that has volume of 0.4 nl. Since the chip has two identical chambers, one of the chambers is used with the template and the other chamber for the control experiment. Fig. 1(a) and 1(b) show a schematic of the device and also a plan view of the actual microchip, respectively. In our experiment, DI water, containing a pre-determined bacterial concentration, was flowed at a desired rate through the main channel and the cells contained within it were deviated by dielectrophoretic (DEP) forces,[12] into a small channel, where the cells were retained by another set of interdigitated electrodes. A maximum flow rate of 0.5 μl min^{-1} could be obtained in the main channel with a peak fluid velocity low enough to guarantee that the DEP forces are sufficient for deviating all the cells from main channel to the small channel. The DEP and diversion electrodes were patterned over 200 nm-thick thermally grown silicon dioxide and covered with a layer of 200 nm-thick PECVD silicon dioxide. The top oxide as well as the cover glass was coated with 0.1 mg ml^{-1} BSA (Sigma, St. Louis, Mo) solution to prevent non-specific adsorption of any protein or nucleic acids. A 20 V_{pp} DEP excitation voltage was used. A thin-film platinum resistor located between the two chambers was used as a temperature sensor. This thin-film resistor was calibrated with a commercially available four-wire thermocouple with a process described later.

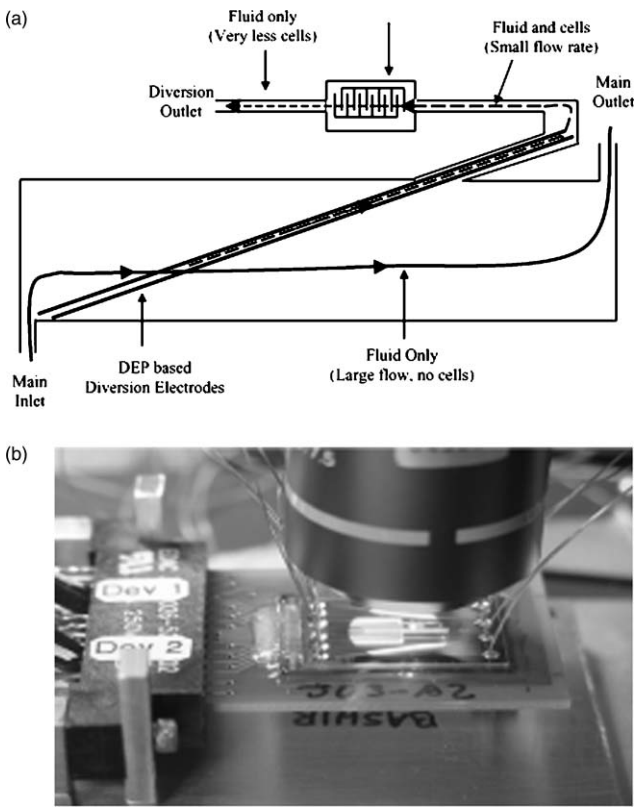

Fig. 1 (a) Principle of operation of the dielectrophoresis-based diversion and capture of cells. (b) Close-up image of the actual device. [Adapted from ref. 12. Copyright 2005, IEEE.]

Packaging and instrumentation

After fabrication, the biochip was fixed onto a custom-designed printed circuit board (PCB) using thermally conductive epoxy. The PCB facilitated the connection of the chip to the equipment that provided the DEP signal, measured and controlled the temperature of the chip. Besides, the PCB contained an integrated heater and also gold-plated bond pads that connect to the pads onto the chip by wire-bonding. The chip was mounted on a stage of an epifluorescence Nikon microscope (Eclipse 600) (see ESI† for details of the control apparatus and the optical detection system). Fig. 2(a) and 2(b) show two microscopic snap-shots of the collection of *L. monocytogenes* ATCC 23074 pNF8 bacterial cells on the DEP diversion and capture electrodes, respectively.

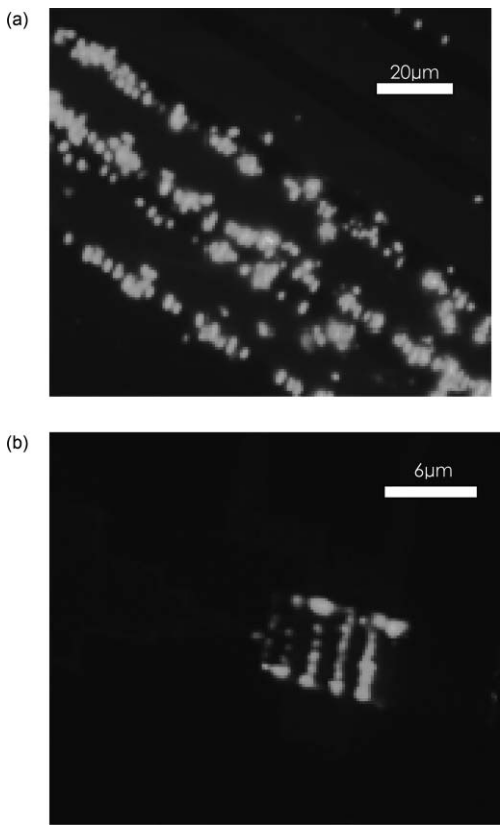

Fig. 2 (a) *L. monocytogenes* ATCC 23074 pNF8 bacterial cells on DEP diversion electrodes, (b) *L. monocytogenes* ATCC 23074 pNF8 bacterial cells on the DEP capture electrodes.

Procedure for PCR on the biochip

In the first set of trials, the bacterial template concentration was varied from 10^4 to 10^8 cfu ml^{-1}, pre-mixed with PCR mix,

and flowed through the chip at 0.5 μl min^{-1} without using DEP concentration. The biochip was imaged using the Nikon microscope mounted with a Pixera CCD camera and the residual fluorescence intensity values were recorded over the chambers using a Photomultiplier Tube (PMT). Fluorescence microscopic images of cells in the chambers were taken after injecting the PCR mix into the chip [see ESI† Fig. S2(a)]. A major drawback of all miniaturized PCR chips has been the inhibition of PCR due to evaporation of the fluid sample during thermal cycling.[21] Various techniques to prevent the evaporation of PCR fluid and bubble formation have been reported by earlier investigators including use of micro-valves,[31] pressurizing the chip using external controls,[32] various surface treatment schemes,[33,34] or usage of mineral oil.[35] In our case, the chip was mounted on the Peltier stage and sealed using an intermediate rubber spacer and a top plate with a metal fixture to prevent analyte evaporation. The chip was then thermally cycled using the instrumentation described earlier, and an end-point fluorescence value was measured.

In the second set of trials, bacterial cultures with similar concentrations were flowed at the same flow rate and a 20 V_{pp} AC signal at frequency of 100 KHz was applied to divert bacterial cells from the main channel into the smaller channel, wherein a set of interdigitated electrodes was used to trap and concentrate the cells. Then the PCR mix was metered into the smaller channel with a syringe pump (Harvard) at a rate of 0.01 μl min^{-1}. Another image of the concentrated *L. monocytogenes* ATCC 23074 pNF8 bacterial cells with DEP-based active trapping was taken after the flow of the PCR mix [see ESI† Fig. S2(b)]. PCR was performed on this sample following an identical protocol as mentioned earlier. The total working volume for capture, lysis, and PCR analysis was only about 600 nl.

Results and discussion

Device calibration and signal plot of the thermal cycle

Before performing experiments on the biochip, the built-in platinum RTD temperature sensor was calibrated, against a commercially available four-wire thermocouple (Omega), by immersing the fully-packaged chip in a heated and stirred DI water bath whose temperature was rising at approximately 0.5 °C min^{-1}. The thermocouple was also immersed in the bath as close to the chip as possible. The RTD and thermocouple were connected to two separate digital multimeters, both of which have GPIB interfaces and were controlled using a LabView program. The temperature of the bath was slowly raised and the temperature *versus* resistance data were plotted. A fit was generated by LabView based on the following eqn (3),

$$R = R_0 + AT + BT^2 \quad (3)$$

where T is the increment in temperature over room temperature, R_0 is the resistance at room temperature, A and B are constant coefficients. The code outputs the iterated values in a matrix form, out of which the final averages were used for controlling the temperature. The parameters R_0, A, and B were obtained as 4.53×10^3 Ω, 2.82×10^{-3}, and -5.74×10^{-6}, respectively. The temperature control code comprised of a PID controller which was balanced using Zeigler–Nichols algorithm.[36] Two different configurations A and B (Fig. 3) were investigated. The first configuration A was exposed to passive cooling in ambient air. The second configuration B was actively cooled by mounting the chip on a Peltier block. The aluminium block was used as a heat sink for the Peltier block. The average heating rate for the passive cooling case (configuration A) was experimentally observed to be about 3.6 °C s^{-1}. The cooling rate for configuration A was measured to be about 1.7 °C s^{-1}. For active cooling, the average heating rate reduced to 3.2 °C s^{-1} and the cooling rate was substantially increased to 5.1 °C s^{-1}. The PCR amplification for *L. monocytogenes* V7 was comprised of 34 cycles, and an overall reduction of 408 s in total cycle time was achieved by the introduction of the forced cooling process. A snap-shot of the thermal cycle with the different temperature and time values is also plotted (see ESI† Fig. S3). The average power used for obtaining the thermal cycle was 2.5 W, although the peak power requirements for heating the chip were around 11–12 W. The fluid loss within the chip was negligible because of the effective sealing using the packaging and clamping fixture as described earlier.

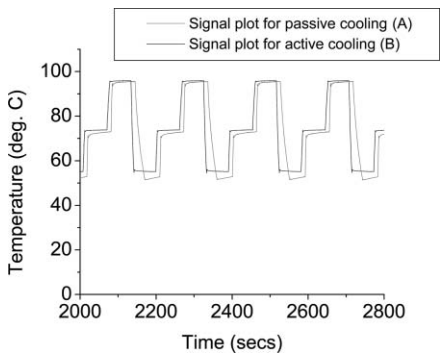

Fig. 3 Thermal cycling profile of passive *versus* active cooling for configurations A and B.

DEP trapping of bacteria

L. monocytogenes ATCC 23074 pNF8, a GFP-producing strain, in either LCGM or resuspended in DI water, were flowed into the micro-channels at various flow rates using off-chip syringe pumps. The signal generators connected to the DEP electrodes (in the main channel and small channel) were switched on. To achieve high capture efficiency of the bacterial cells, the DEP forces had to be strong enough so as to overcome the drag forces exerted by the flowing fluid. Our earlier work shows that the *Listeria* cells, suspended in DI water (conductivity of 1 μS cm^{-1}), experience a very strong positive DEP force, at an excitation frequency of 100 kHz. Under these conditions the cells are directed to the region of the electrode having the highest field gradient (positive DEP), so that the cells collect on the edge of the electrode. Fig. 2(a) shows the *L. monocytogenes* ATCC 23074 pNF8 cells being captured over the diversion electrodes that direct the cell flow from the main channel towards the small channel. Fig. 2(b) shows the capture of the bacterial cells inside the smaller 0.4 nl chamber with DEP on. In order to obtain maximum capture (approx. 100% capture efficiency), the correct combination of the medium conductivity, flow velocities, DEP excitation voltage and frequency must be used. We observe a

maximum diversion and capture efficiency at a flow rate of 0.5 µl min^{-1}, a DEP voltage of 20 V_{pp} and a frequency of 100 kHz. The total numbers of cells that were injected into the biochip, without any active trapping, are a function of the total chip volume (0.6 µl) and the flow rate. Such as, if the sample solution with the concentration of 10^8, 10^7, 10^6, 10^5, and 10^4 cfu ml^{-1} is flowed, for 1.2 min, at the flow rate of 0.5 µl min^{-1}, the number of cells, in 0.6 µl volume of the chip, are estimated to be 60 000, 6000, 600, 60, and 6 cells, respectively.

PCR protocol

The PCR protocol was verified with DNA amplification and standard gel electrophoresis. The optical density (OD) of this culture was balanced to 0.50–0.55 (by diluting in BHI). This OD corresponds to a concentration of 10^9 cfu ml^{-1},[36] which was evaluated by plating on BHI agar. 5 µl of the cell suspension was lysed using a hot water bath [containing near-boiling water (90 °C)] for 17–18 min. A q-PCR kit (Invitrogen) was used to amplify the extracted template and the gel electrophoresis technique was used to confirm the amplification. It was noted that using this protocol we could successfully perform off-chip PCR for the cell concentrations ranging from approx. 10^8 to 10^3cfu ml^{-1}. Fig. 4 shows a post-PCR gel image of the serial dilutions.

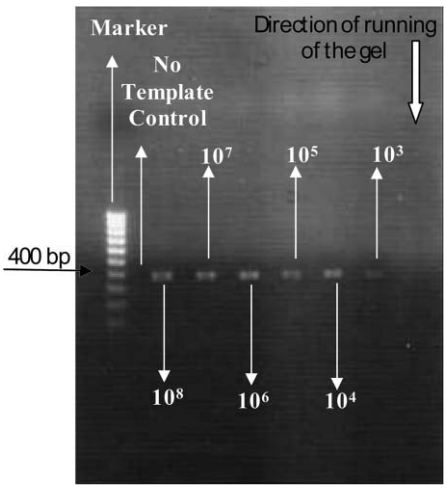

Fig. 4 One-dimensional gel electrophoresis for post-PCR samples with varying concentrations of bacterial cells (from 10^3 to 10^8 cfu ml^{-1}).

PCR on a chip

On-chip trials, for different concentrations of *L. monocytogenes* V7, were performed and the fluorescence values were recorded before and after the thermal cycling. These fluorescence values were taken at multiple points on the chip and their averages and standard deviations were computed and plotted as a bar graph (see ESI† Fig. S4). An error bar, indicating the standard deviation in the fluorescence readings for each concentration, is also added to the average fluorescence bar graph. Fig. 5 summarizes the different fluorescence values obtained for the trials performed without DEP. Trial 1 fluorescence values correspond to no-template control (no cells but all components of the PCR reaction). All fluorescence values were normalized with

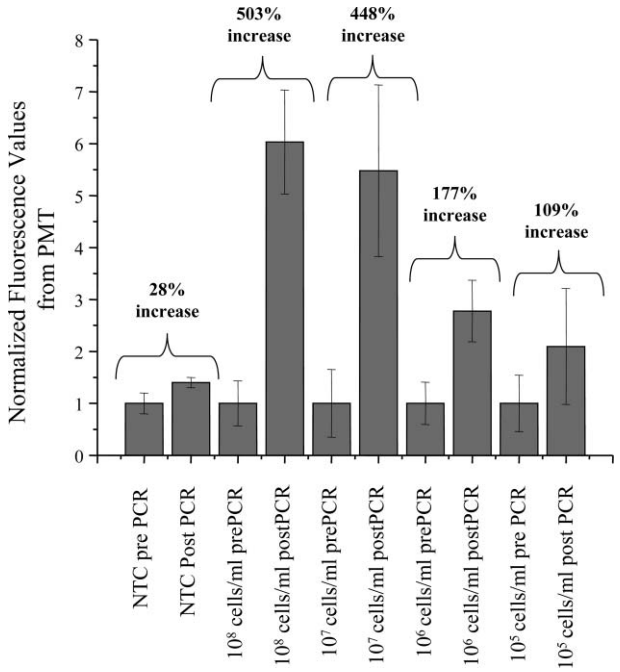

Fig. 5 Pre- and post-PCR summary of fluorescence data for various cell concentrations without any active DEP concentration.

respect to a baseline. As seen in the average fluorescence plot, for the no-template control, a 28% increase in the fluorescence was recorded which could be attributed to the formation of primer-dimers intercalating with SYBR Green dye molecules. For the 10^8 cfu ml^{-1}, the increase in fluorescence of the post PCR products was 503%. Similarly, for 10^7 cfu ml^{-1}, the increase was 448% and for 10^6 cfu ml^{-1}, the increase was 177%. For 10^5 cfu ml^{-1} (corresponding to 60 cells) the average increase in fluorescence was 109% and the normalized fluorescence values of pre- and post-PCR were 1.0 ± 0.4 (pre-PCR) and 2.1 ± 1.1 (post-PCR). The minimum number of cells that could provide a nearly measurable signal was found to be 60. With a flow rate of 0.5 µl min^{-1} and 100% capture efficiency,[12] 500 cells can be trapped inside the chip in one minute, from a concentration of 10^6 cfu ml^{-1}. Similarly, 50 and 5 cells can be trapped in one minute from a concentration of 10^5 and 10^4 cfu ml^{-1} respectively. In order to achieve the minimum detectable limit of the system, DEP-based concentration was performed in the chip and dilutions ranging from about 10^5–10^4 cfu ml^{-1} were investigated. Fig. 6(a) shows that with the DEP-based concentration, the average fluorescence increase in the chamber for the concentration of 10^5 cfu ml^{-1} was about 339%, and the normalized fluorescence values were 1.0 ± 0.5 and 4.3 ± 0.4 for the pre- and post-PCR samples, respectively. As discussed earlier, this is a marked improvement compared to the trial done without DEP for the same concentration (10^5 cfu ml^{-1}), wherein, though the average increase in fluorescence was around 109%, the normalized fluorescence values before and after PCR were very close to each other. When using the concentration of 10^4 cfu ml^{-1} along with DEP, the post-PCR increase in fluorescence was observed to be 220%. The normalized fluorescence values vary in this case from 1.0 ± 0.4 in pre-PCR solution to 3.2 ± 0.68 in the post-PCR product. As stated earlier, the

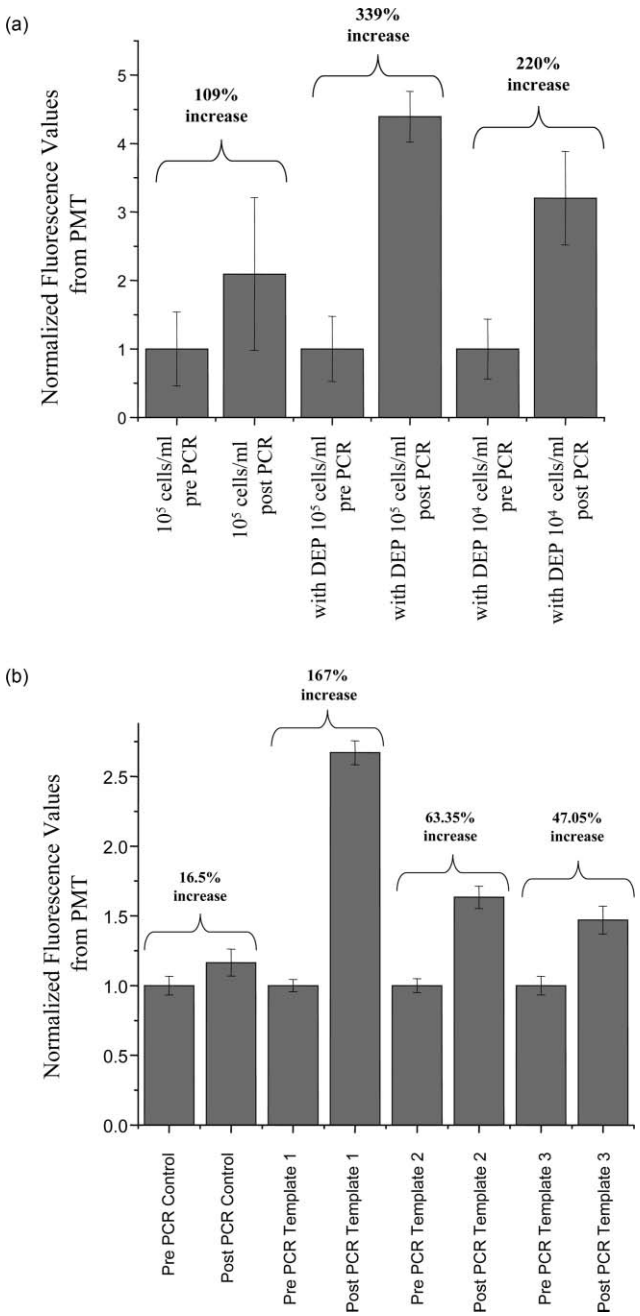

Fig. 6 (a) Pre- and post-PCR summary data with DEP concentration. (b) Specificity trials for *L. monocytogenes* V7 with concentrations of 10^8, 10^7 and 10^6 cfu ml^{-1} sample comprising a 1 : 1 : 1 mixture of *L. monocytogenes* V7, *L. innocuo* F4248 and *E. coli* H157:O7 as the starting template. The control sampled comprised a 1 : 1 mixture of *L. innocuo* F4248 and *E. coli* H157:O7 as the starting template.

concentration of 10^4 cfu ml^{-1} was not detectable without DEP-based concentration.

Specificity trials

L. monocytogenes V7 was used for on-chip DEP and PCR trials, while *L. innocua* F4248, and *E. coli* O157:H7 were used for the specificity testing of our protocol. In these trials, a mixture of approx. 10^8–10^6 cfu ml^{-1} *L. monocytogenes* V7, 10^8 cfu ml^{-1} *L. innocua* F4248, and 10^8 cfu ml^{-1} *E. coli* O157:H7 were mixed in equal proportions. The primers used in these trials are highly specific to *L. monocytogenes* V7, and result in amplification of the 508 bp region of the *prfa* gene. The control sample consisted of *L. innocua* F4248 and *E. coli* O157:H7 alone. Fig. 6(b) illustrates the various normalized fluorescence values using the three cell mixtures. For the control sample the normalized fluorescence signal, after thermal cycle, increases by 16%. For the 10^8 cfu ml^{-1} *L. monocytogenes* V7, *L. innocua* F4248, and *E. coli* O157:H7 (1 : 1 : 1) mixture, the increase in normalized fluorescence was 167%. For 10^7 and 10^6 cfu ml^{-1} of *L. monocytogenes*, and 10^8 cfu ml^{-1} *L. innocua* F4248, and *E. coli* O157:H7 (1 : 1 : 1) the recorded increase in fluorescence was 63 and 47% respectively. If we compare these values with the earlier ones involving one cell type (*L. monocytogenes* V7), we find a considerable decrease in the fluorescence values. The lower fluorescence signal in the case of specificity trials may be due to a decrease in the initial available template in this case to 33.33% (one-third) and due to other DNA sequences from *L. innocua* F4248, and *E. coli* O157:H7 that can compete for the total available PCR reactants, thus lowering the amplification efficiency. However, the increase of fluorescence is a positive indication of the presence of *L. monocytogenes* V7.

Conclusions

A fully integrated microfluidic system to concentrate, and analyze nanoliter volumes of DNA and detect *L. monocytogenes* V7 using PCR amplification, with high specificity, has been demonstrated. The system has integrated micro-fabricated heating and temperature sensing elements and these elements significantly improve the thermal cycling efficiency and heating and cooling rates. This integrated micro-system is capable of detecting 60 cells of *L. monocytogenes* V7 within a 600 nl volume. Moreover, utilizing DEP, an increase in the sensitivity of detection, from 10^6 to 10^4 cfu ml^{-1} is achieved.

References

1 S. S. Iqbal, M. W. Mayo, J. G. Bruno, B. V. Bronk, C. A. Batt and J. P. Chambers, *Biosens. Bioelectron.*, 2000, **15**, 549–578.
2 M. G. Giminska, *Microbial Cell Factories*, 2006, **5**, 1–8.
3 M. Ramsey, *Nat. Biotechnol.*, 1998, **16**, 40–49.
4 C. F. Edman, P. Mehta, R. Press, C. A. Spargo, G. T. Walker and M. Nererberg, *J. Invest. Med.*, 2000, **48**, 93–101.
5 T. M. H. Lee, M. C. Carles and I. M. Hsig, *Lab Chip*, 2003, **3**, 100–105.
6 E. T. Lagally, P. C. Simpson and R. A. Mathies, *Sens. Actuators, B*, 2000, **63**, 138–146.
7 D. V. Lim, T. M. Simpson, E. A. Kearns and M. F. Kramer, *Clin. Microbiol. Rev.*, 2005, **18**, 583–607.
8 J. P. Natero and J. B. Kaper, *Clin. Microbiol. Rev.*, 1998, **11**, 192–197.
9 D. Y. C. Fung, *IFT Electronic J.*, 2002, **1**, 3–22.
10 M. J. Payne and D. G. Knull, *Trends Food Sci. Technol.*, **2**, 315–319.
11 H. Y. Hsieh and H. Y. Tsen, *J. Food Prot.*, 2001, **64**, 1744–1750.
12 R. Gomez-Sjoberg, D. M. Morisette and R. Bashir, *J. Microelectromech. Syst.*, 2005, **14**, 829–838.
13 C. R. Cabrera and P. Yeager, *Electrophoresis*, 2001, **22**, 355–382.
14 X. Hu, P. H. Bessette, J. Qian, C. D. Meinhart, P. S. Daugherty and T. H. Soh, *Proc. Natl. Acad. Sci. U. S. A.*, **102**, 15757–15761.
15 P. Grodinzki, J. Yang, D. H. Liu and M. D. Ward, *Biomed. Microdevices*, 2003, **5**, 303–310.
16 K. Handique, D. T. Burke, C. H. Mastrangello and M. A. Burns, *Anal. Chem.*, 2002, **72**, 4100–4109.
17 R. A. Mathies, P. C. Simpson and S. J. Williams, *US Pat.*, 6261431 B1, 2001.

18 J. L. Bono, J. E. Keen, L. C. Miller, J. M. Fox, C. G. C. McKown, M. P. Heaton and W. W. Laegreid, *Appl. Environ. Microbiol.*, 2004, **70**, 1855–1857.
19 T. Notomi, H. Okayama, H. Masubuchi, T. Yonekawa, K. Watanabe, N. Amino and T. Hase, *Nucleic Acids Res.*, 2000, **28**, E63.
20 C. S. Hill, *Expert Rev. Mol. Diagnostics*, 2000, **1**, 445–455.
21 C. Zhang and D. Xing, *Nucleic Acids Res.*, 2007, **35**, 4223–4237.
22 I. D. R. Neilsen, D. D. Bag, C. R. Poulsen, J. E. Ali and A. Wolf, *Lab Chip*, 2003, **3**, 212–216.
23 B. Alberts, A. Johnson, J. Lewis, M. Raff, K. Roberts, P. Walter and G. Sand, *Molecular Biology of the Cell*, Taylor and Francis group, Boca Raton, FL, 4th edn, 2002 .
24 E. T. Lagally, S. H. Lee and H. T. Soh, *Lab Chip*, 2005, **5**, 1053–1058.
25 Y. Huang, R. Holzel, R. Pethig and X. B. Wang, *Phys. Med. Biol.*, 1992, **37**, 1499–1517.
26 H. A. Pohl, *J. Appl. Phys.*, 1951, **22**, 869–871.
27 X. B. Wang, Y. Huang, J. P. H. Burt, G. H. Markx and R. Pethig, *J. Phys. D: Appl. Phys.*, 1999, **26**, 1278–1285.
28 B. H. L. Encinas, B. A. Simmons, E. B. Cummings and Y. Fintschenko, *Electrophoresis*, 2004, **25**, 1695–1704.
29 L. Yang, P. P. Banada, Y. Liu, A. K. Bhunia and R. Bashir, *Biotechnol. Bioeng.*, 2005, **92**, 685–694.
30 P. G. Klein and V. K. Juneja, *Appl. Environ. Microbiol.*, 1997, **63**, 4441–4448.
31 Y. S. Shin, K. Cho, S. H. Lim, S. Chung, S. J. Park, C. Chung, D. C. Han and J. K. Chang, *J. Micromech. Microeng.*, 2003, **13**, 768–774.
32 J. W. Hong, T. Fujii, M. Seki, T. Yamamoto and I. Endo, *Electrophoresis*, 2001, **22**, 328–333.
33 J. Cheng, M. A. Shoffner, G. E. Hvichia, L. J. Kricka and P. Wilding, *Nucleic Acids Res.*, 1996, **24**, 380–385.
34 S. Bhattacharya, Y. Gao, V. Korampally, M. T. Othman, S. A. Grant, S. B. Kleiboeker, K. Gangopadhyay and S. Gangopadhyay, *J. Microelectromech. Syst.*, 2007, **16**, 401–410.
35 M B Coyne, *Phys. Med. Biol.*, 1974, **19**, 708–715.
36 B. G. Liptak, *Instrument Engineers Handbook, Process Control*, CRC Press, Taylor and Francis Group, Boca Raton, NY, 3rd edn, 1999.

